

---

# Augmentation-Aware Self-Supervision for Data-Efficient GAN Training

---

Liang Hou<sup>1,3</sup>, Qi Cao<sup>1</sup>, Yige Yuan<sup>1,3</sup>, Songtao Zhao<sup>4</sup>, Chongyang Ma<sup>4</sup>,  
Siyuan Pan<sup>4</sup>, Pengfei Wan<sup>4</sup>, Zhongyuan Wang<sup>4</sup>, Huawei Shen<sup>1,3</sup>, Xueqi Cheng<sup>2,3</sup>

<sup>1</sup>Data Intelligence System Research Center,  
Institute of Computing Technology, Chinese Academy of Sciences  
<sup>2</sup>CAS Key Laboratory of Network Data Science and Technology,  
Institute of Computing Technology, Chinese Academy of Sciences  
<sup>3</sup>University of Chinese Academy of Sciences <sup>4</sup>Kuaishou Technology  
{houliang17z, caoqi, yianyige20z, shenhuawei, cxq}@ict.ac.cn

## Abstract

Training generative adversarial networks (GANs) with limited data is challenging because discriminator is prone to overfitting. Previously proposed differentiable augmentation demonstrates improved data efficiency of training GANs. However, the augmentation implicitly introduces undesired invariance to augmentation for the discriminator since it ignores the change of semantics in the label space caused by data transformation, which may limit the representation learning ability of the discriminator and ultimately affect the generative modeling performance of the generator. To mitigate the negative impact of invariance while inheriting the benefits of data augmentation, we propose a novel augmentation-aware self-supervised discriminator that predicts the augmentation parameter of the augmented data. Particularly, the prediction targets of real data and generated data are required to be distinguished since they are different during training. We further encourage the generator to adversarially learn from the self-supervised discriminator by generating augmentation-predictable real but not fake data. This formulation connects the learning objective of the generator and the arithmetic–harmonic mean divergence under certain assumptions. We compare our method with state-of-the-art (SOTA) methods using the class-conditional BigGAN and unconditional StyleGAN2 architectures on data-limited CIFAR-10, CIFAR-100, FFHQ, LSUN-Cat, and five low-shot datasets. Experimental results demonstrate significant improvements of our method over SOTA methods in training data-efficient GANs.<sup>1</sup>

## 1 Introduction

Generative adversarial networks (GANs) [9] have achieved great progress in synthesizing diverse, high-quality images in recent years [2, 18, 19, 17, 11]. However, the generation quality of GANs depends heavily on the amount of training data [45, 16]. In general, the decrease of training samples usually yields a sharp decline in both fidelity and diversity of the generated images [37, 46]. This hinders the wide application of GANs due to the fact of insufficient data in real-world applications. For instance, it is valuable to imitate the style of an artist whose paintings are limited. GANs typically consist of a generator that is designed to generate new data and a discriminator that guides the generator to recover the real data distribution. The major challenge of training GANs under limited data is that the discriminator is prone to overfitting [45, 16], and therefore lacks generalization to teach the generator to learn the underlying real data distribution.

---

<sup>1</sup>Our code is available at <https://anonymous.4open.science/r/augself-gan>.

In order to alleviate the overfitting issue, recent researches have suggested a variety of approaches, mainly from the perspectives of training data [16], loss function [38], and network architecture [26] (see Section 2.1 for detailed discussion). Among them, data augmentation-based methods have gained widespread attention due to its simplicity and extensibility. Specifically, DiffAugment [45] introduced differentiable augmentation techniques for GANs, in which both real and generated data are augmented to supplement the training set of the discriminator. However, this straightforward augmentation method overlooks augmentation-related semantic information, as it solely augments the domain of the discriminator while neglecting the codomain. Such a practice might introduce an inductive bias that potentially forces the discriminator to remain invariant to different augmentations [23], which could limit the representation learning of the discriminator and subsequently affect the generation performance of the generator [12].

In this paper, we propose a novel augmentation-aware self-supervised discriminator that predicts the augmentation parameter of augmented data with the original data as reference to address the above problem. Meanwhile, the self-supervised discriminator is required to be distinguished between the real data and the generated data since their distributions are different during training, especially in the early stage. The proposed discriminator can benefit the generator in two ways, implicitly and explicitly. On one hand, the self-supervised discriminator can transfer the learned augmentation-aware knowledge to the original discriminator through parameter sharing. On the other hand, we allow the generator to learn adversarially from the self-supervised discriminator by generating augmentation-predictable real but not fake data. We also theoretically analyzed the connection between this objective function and the minimization of a robust  $f$ -divergence divergence (the arithmetic–harmonic mean divergence [35]). In experiments, we show that the proposed method significantly outperforms the data augmentation counterparts and other state-of-the-art methods on common data-limited benchmarks (CIFAR-10, CIFAR-100 [20], FFHQ [18], LSUN-Cat [43], and five low-shot datasets [34]) based on the class-conditional BigGAN [2] and unconditional StyleGAN2 [19] architectures. In addition, we carried out extensive experiments to demonstrate the effectiveness of the objective function design, the adaptability to stronger data augmentations, and the robustness of hyper-parameter selection in our method.

## 2 Related Work

In this section, we provide an overview of the existing work related to training GANs in data-limited scenarios, and we also discuss methodologies incorporating self-supervised learning techniques.

### 2.1 GANs under Limited Training Data

Recently, researchers have become interested in freeing training GANs from the need to collect large amounts of data for adaptability in real-world scenarios. Previous studies typically fall into two main categories. The first one involves adopting a pre-trained GAN model to the target domain by fine-tuning partial parameters [40, 29, 39, 28]. However, this requires external training data, and the adoption performance depends heavily on the correlation between the source and target domains.

The other one focuses on training GANs from scratch with elaborated data-efficient training strategies. DiffAugment [45] utilized differentiable augmentation to supplement the training set to prevent discriminator from overfitting in limited data regimes. Concurrently, ADA [16] introduced adaptive data augmentation with a richer set of augmentation categories. APA [15] adaptively augmented the real data with the most plausible generated data. LeCam-GAN [38] proposed adaptive regularization for the discriminator and show a connection to the Le Cam divergence [22]. [3] discovered that sparse sub-network (lottery tickets) [5] and feature-level adversarial augmentation could offer orthogonal gains to data augmentation methods. InsGen [41] improved the data efficiency of training GANs by incorporating instance discrimination tasks to the discriminator. MaskedGAN [13] employed masking in the spatial and spectral domains to alleviate the discriminator overfitting issue. GenCo [6] discriminated samples from multiple views with weight-discrepancy and data-discrepancy mechanisms. FreGAN [42] focused on discriminating between real and fake samples in the high-frequency domain. DigGAN [7] constrains the discriminator gradient gap between real and generated data. FastGAN [26] designed lightweight generator architecture and observed that a self-supervised discriminator could enhance low-shot generation performance. Our method falls into the second category, supplementing data augmentation-based GANs and can also be applied to other methods (as future work).

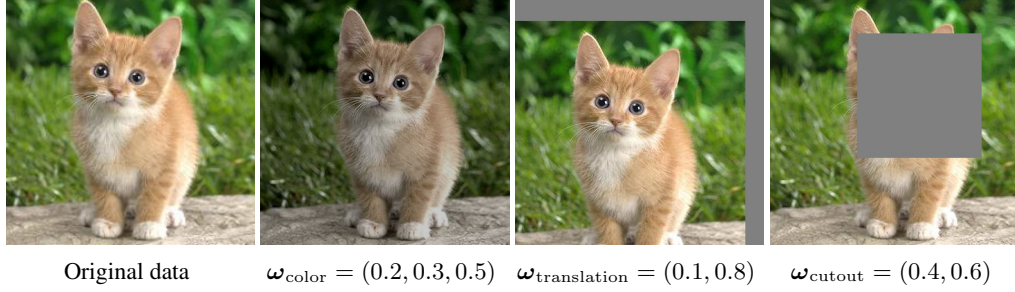


Figure 1: Examples of images with different kinds of differentiable augmentation (including the original unaugmented one) and their re-scaled corresponding augmentation parameters  $\omega \in [0, 1]^d$ .

## 2.2 GANs with Self-Supervised Learning

Self-supervised learning techniques excel at learning meaningful representations without human-annotated labels by solving pretext tasks. Transformation-based self-supervised learning methods such as rotation recognition [8] have been incorporated into GANs to address catastrophic forgetting in discriminator [4, 36, 12]. Various other self-supervised tasks have also been explored, including jigsaw puzzle solving [1], latent transformation detection [31], and mutual information maximization [24]. Moreover, ContraD [14] decouples the representation learning and discrimination of the discriminator, utilizing contrastive learning for representation learning and a discriminator head for the distinguishing real from fake upon the contrastive representations. In contrast to ours, CR-GAN [44] and ICR-GAN proposed consistency regularization for the discriminator, which corresponds to an explicit augmentation-invariant of the discriminator. The proposed method in this paper shares similarities with SSGAN-LA [12], but is different from the form of self-supervised signals. SSGAN-LA is limited to categorical self-supervision such as 90-degree-based rotation recognition [8], which is not typically used in the popular augmentation-based GANs, i.e., DiffAugment [45]. SSGAN-LA aims at mitigating catastrophic forgetting of discriminator and improve the training stability of GANs [4]. In comparison, Our method is applicable for continuous self-supervision and integrates seamlessly with DiffAugment, leading to significantly improved data efficiency of training GANs.

## 3 Preliminaries

In this section, we introduce the necessary concepts and preliminaries for completeness of the paper.

### 3.1 Generative Adversarial Networks

Generative adversarial networks (GANs) [9] typically contain a generator  $G : \mathcal{Z} \rightarrow \mathcal{X}$  that maps a low-dimensional latent code  $\mathbf{z} \in \mathcal{Z}$  endowed with a tractable prior  $p(\mathbf{z})$ , e.g., multivariate normal distribution  $\mathcal{N}(\mathbf{0}, \mathbf{I})$ , to a high-dimensional data point  $\mathbf{x} \in \mathcal{X}$ , which induce a generated data distribution  $p_G(\mathbf{x}) = \int_{\mathcal{Z}} p(\mathbf{z}) \delta(\mathbf{x} - G(\mathbf{z})) d\mathbf{z}$  with the Dirac delta distribution  $\delta(\cdot)$ , and also contain a discriminator  $D : \mathcal{X} \rightarrow \mathbb{R}$  that is required to distinguish between the real data sampled from the underlying data distribution  $p_{\text{data}}(\mathbf{x})$  and the generated data. The generator attempts to fool the discriminator to eventually recover the real data distribution, i.e.,  $p_G(\mathbf{x}) = p_{\text{data}}(\mathbf{x})$ . Formally, the loss functions for the discriminator and the generator can be formulated as follows:

$$\mathcal{L}_D = \mathbb{E}_{\mathbf{x} \sim p_{\text{data}}(\mathbf{x})} [f(D(\mathbf{x}))] + \mathbb{E}_{\mathbf{z} \sim p(\mathbf{z})} [h(D(G(\mathbf{z})))] \quad (1)$$

$$\mathcal{L}_G = \mathbb{E}_{\mathbf{z} \sim p(\mathbf{z})} [g(D(G(\mathbf{z})))] \quad (2)$$

Different real-valued functions  $f$ ,  $h$ , and  $g$  correspond to different variants of GANs [30]. For example, the minimax GAN [9] can be constructed by setting  $f(x) = -\log(\sigma(x))$  and  $h(x) = -g(x) = -\log(1 - \sigma(x))$  with the sigmoid function  $\sigma(x) = 1/(1 + \exp(-x))$ . In this study, we follow the practices of DiffAugment [45] to adopt the hinge loss [25], i.e.,  $f(x) = h(-x) = \max(0, 1 - x)$  and  $g(x) = -x$ , for experiments based on BigGAN [2] and the log loss [9], i.e.,  $f(x) = g(x) = -\log(\sigma(x))$  and  $h(x) = -\log(1 - \sigma(x))$ , for experiments based on StyleGAN2 [19].

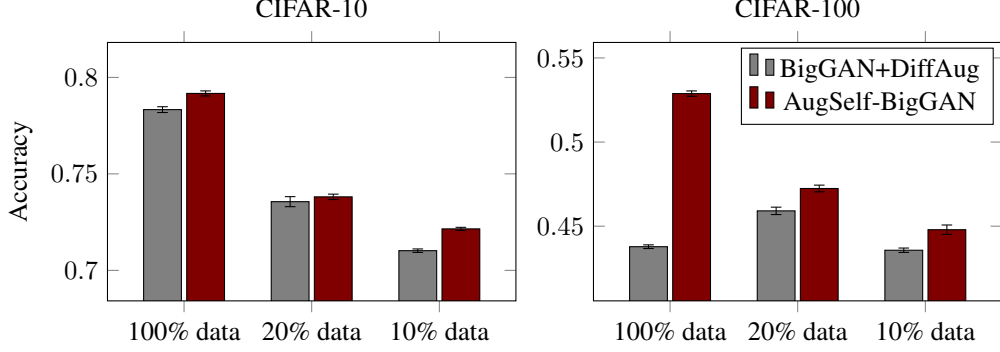


Figure 2: Comparison of representation learning ability of discriminator between BigGAN + DiffAugment and our AugSelf-BigGAN on CIFAR-10 and CIFAR-100 using linear logistic regression.

### 3.2 Differentiable Augmentation for GANs

DiffAugment [45] introduces differentiable augmentation  $T : \mathcal{X} \times \Omega \rightarrow \hat{\mathcal{X}}$  parameterized by a randomly-sampled parameter  $\omega \in \Omega$  with a prior  $p(\omega)$  for data-efficient GAN training. The parameter  $\omega$  determines exactly how to transfer a data  $\mathbf{x}$  to an augmented data  $\hat{\mathbf{x}} \in \hat{\mathcal{X}}$  for the discriminator. After our manually re-scaling (for  $\omega \in [0, 1]^d$ ), the parameters of all three kinds of differentiable augmentation used in DiffAugment for 2D images can be expressed as follows:

- color:  $\omega_{\text{color}} = (\lambda_{\text{brightness}}, \lambda_{\text{saturation}}, \lambda_{\text{contrast}}) \in [0, 1]^3$ ;
- translation:  $\omega_{\text{translation}} = (x_{\text{translation}}, y_{\text{translation}}) \in [0, 1]^2$ ;
- cutout:  $\omega_{\text{cutout}} = (x_{\text{offset}}, y_{\text{offset}}) \in [0, 1]^2$ .

Figure 1 illustrates the augmentations and their parameters. Formally, the loss functions for the discriminator and the generator of GANs with DiffAugment are defined as follows:

$$\mathcal{L}_D^{\text{da}} = \mathbb{E}_{\mathbf{x} \sim p_{\text{data}}(\mathbf{x}), \omega \sim p(\omega)} [f(D(T(\mathbf{x}; \omega)))] + \mathbb{E}_{\mathbf{z} \sim p(\mathbf{z}), \omega \sim p(\omega)} [h(D(T(G(\mathbf{z}); \omega)))] \quad (3)$$

$$\mathcal{L}_G^{\text{da}} = \mathbb{E}_{\mathbf{z} \sim p(\mathbf{z}), \omega \sim p(\omega)} [g(D(T(G(\mathbf{z}); \omega)))] \quad (4)$$

where  $\omega$  can represent any combination of these parameters. We choose all augmentations by default, which means augmentation color, translation, and cutout are adopted for each image sequentially.

## 4 Method

Data augmentation for GANs allows the discriminator to distinguish a single sample from multiple perspectives by transforming it into various augmented samples based on different augmentation parameters. However, data augmentation always overlooks the differences in augmentation intensity, such as color contrast and translation degree, leading the discriminator to implicitly maintain invariance to these varying intensities. This invariance may limit the representation learning ability of the discriminator because it loses augmentation-related information (e.g., color and position) [23]. Figure 2 confirms the impact of this point on the discriminator representation learning. We believe that a discriminator that captures comprehensive representations contributes to better convergence of the generator [33, 21]. Moreover, data augmentation may lead to augmentation leaking in generated data, when using specific data augmentations such as random 90 degree rotations [16, 12]. Therefore, our goal is to eliminate the unnecessary potential inductive bias (invariance to augmentation) for the discriminator while preserving the benefits of data augmentation for training data-efficient GANs.

To achieve this goal, we propose a novel augmentation-aware self-supervised discriminator  $\hat{D} : \hat{\mathcal{X}} \times \mathcal{X} \rightarrow \Omega^+ \cup \Omega^-$  that predicts the augmentation parameter and the realness of the augmented data given the original data as reference. Distinguishing between the real data and the generated data with different self-supervision is because they are different during training, especially in the early stage. Specifically, the predictive targets of real data and generated data are represented as  $\omega^+ \in \Omega^+$  and  $\omega^- \in \Omega^-$ , respectively. They are constructed from the augmentation parameter  $\omega$  with different transformations, i.e.,  $\omega^+ = -\omega^- = \omega$ . Since the augmentation parameter is a



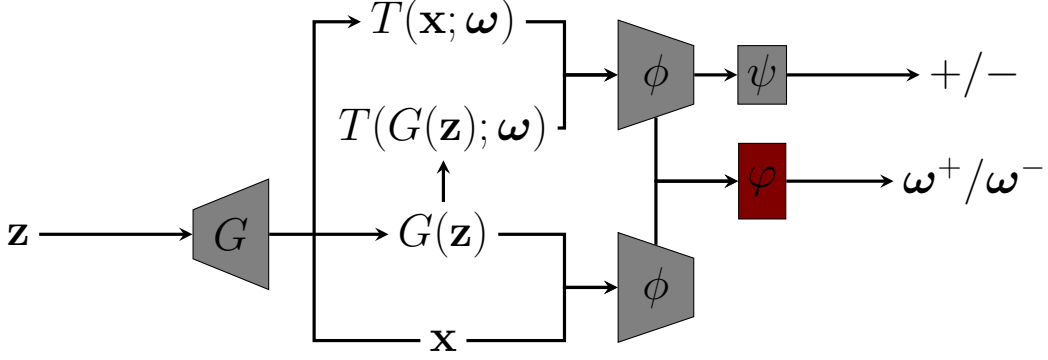


Figure 3: Diagram of AugSelf-GAN. The original augmentation-based discriminator is  $D(T(\cdot)) = \psi(\phi(T(\cdot)))$ . The augmentation-aware self-supervised discriminator is  $\hat{D}(T(\cdot), \cdot) = \varphi(\phi(T(\cdot)) - \phi(\cdot))$ , where  $\varphi$  is our newly introduced linear layer with negligible additional parameters.

continuous vector, we use mean squared error loss to regress it. The proposed method combines continuous self-supervised signals with real-vs-fake discrimination signals, thus can be considered as soft-label augmentation [12] (see Table 6 in Appendix B for comparison with alternative forms of self-supervised tasks). Notice that the predictive targets (augmentations) can be a subset of performed augmentations (see Table 7 in Appendix B for empirical comparison). Mathematically, the loss function for the augmentation-aware self-supervised discriminator is formulated as the following:

$$\mathcal{L}_D^{ss} = \mathbb{E}_{\mathbf{x}, \omega} [\|\hat{D}(T(\mathbf{x}; \omega), \mathbf{x}) - \omega^+\|_2^2] + \mathbb{E}_{\mathbf{z}, \omega} [\|\hat{D}(T(G(\mathbf{z}); \omega), G(\mathbf{z})) - \omega^-\|_2^2]. \quad (5)$$

In our implementations, the proposed self-supervised discriminator  $\hat{D} = \varphi \circ \phi$  shares backbone  $\phi : \mathcal{X} \rightarrow \mathbb{R}^d$  with the original discriminator  $D = \psi \circ \phi$  except the output linear layer  $\varphi : \mathbb{R}^d \rightarrow \Omega^+ \cup \Omega^-$ . This parameter-sharing design not only improves the representation learning ability of the original discriminator but also saves the number of parameters in our model compared to the base model, e.g., 0.04% more parameters in BigGAN and 0.01% in StyleGAN2. More specifically, the discriminator predicts the target based on the difference between learned representations of the augmented data and the original data, i.e.,  $\hat{D}(T(\mathbf{x}; \omega), \mathbf{x}) = \varphi(\phi(T(\mathbf{x}; \omega)) - \phi(\mathbf{x}))$  (see Table 8 in Appendix B for comparison with other architectures). The philosophy behind our design is that the backbone  $\phi$  should capture rich (which necessitates the design of a simple head  $\varphi$ ) and disentangled (inspiring us to perform subtraction on the features) representations.

In order for the generator to directly benefit from the self-supervision of data augmentation, we establish a novel adversarial game between the augmentation-aware self-supervised discriminator and the generator with the following objective function for the generator defined as follows:

$$\mathcal{L}_G^{ss} = \mathbb{E}_{\mathbf{z}, \omega} [\|\hat{D}(T(G(\mathbf{z}); \omega), G(\mathbf{z})) - \omega^+\|_2^2] - \mathbb{E}_{\mathbf{z}, \omega} [\|\hat{D}(T(G(\mathbf{z}); \omega), G(\mathbf{z})) - \omega^-\|_2^2]. \quad (6)$$

The objective function is the combination of the non-saturating loss (regards the generated data as real,  $\min_G \mathbb{E}_{\mathbf{z}, \omega} [\|\hat{D}(T(G(\mathbf{z}); \omega), G(\mathbf{z})) - \omega^+\|_2^2]$ ) and the saturating loss (reversely optimizes the objective function of the discriminator,  $\max_G \mathbb{E}_{\mathbf{z}, \omega} [\|\hat{D}(T(G(\mathbf{z}); \omega), G(\mathbf{z})) - \omega^-\|_2^2]$ ) (see Table 9 in Appendix B for analysis). Intuitively, the non-saturating loss encourages the generator to produce augmentation-predictable data, facilitating fidelity but reducing diversity. Conversely, the saturating loss strives for the generator to avoid generating augmentation-predictable data, promoting diversity at the cost of fidelity. We will elucidate in Section 5 how this formalization assists the generator in matching the fidelity and diversity of real data, ultimately leading to an accurate approximation of the target data distribution.

The total objective functions for the discriminator, the augmentation-aware self-supervised discriminator, and the generator of our proposed method, named AugSelf-GAN, are given by:

$$\min_{D, \hat{D}} \mathcal{L}_D^{da} + \lambda_d \cdot \mathcal{L}_D^{ss}, \quad (7)$$

$$\min_G \mathcal{L}_G^{da} + \lambda_g \cdot \mathcal{L}_G^{ss}. \quad (8)$$

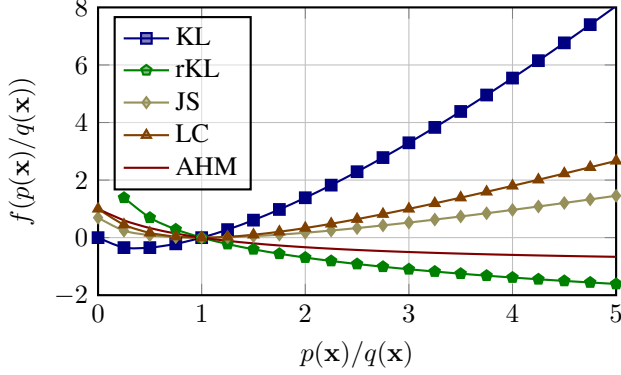


Figure 4: Comparison of the function  $f$  in different  $f$ -divergences. The  $f$ -divergence between two probability distributions  $p(\mathbf{x})$  and  $q(\mathbf{x})$  is defined as  $D_f(p(\mathbf{x})\|q(\mathbf{x})) = \int_{\mathcal{X}} q(\mathbf{x}) f(p(\mathbf{x})/q(\mathbf{x})) d\mathbf{x}$  with a convex function  $f : \mathbb{R}_{\geq 0} \rightarrow \mathbb{R}$  satisfying  $f(1) = 0$ . The x- and y-axis denote the input and the value of the function  $f$  in the  $f$ -divergence. The function  $f$  of the AHM divergence yields the most robust value for large inputs.

We set the hyper-parameters as  $\lambda_d = \lambda_g = 1$  in our experiments by default unless otherwise specified (see Figure 5 for empirical analysis).

## 5 Theoretical Analysis

In this section, we explore the connection between the theoretical learning objective of the generator of AugSelf-GAN and the arithmetic–harmonic mean divergence [35] under certain assumptions.

**Proposition 1.** *For any generator  $G$  and given unlimited capacity in the function space, the optimal augmentation-aware self-supervised discriminator  $\hat{D}^*$  has the form of:*

$$\hat{D}^*(\hat{\mathbf{x}}, \mathbf{x}) = \frac{\int p_{\text{data}}(\mathbf{x}, \omega, \hat{\mathbf{x}}) \omega^+ d\omega + \int p_G(\mathbf{x}, \omega, \hat{\mathbf{x}}) \omega^- d\omega}{p_{\text{data}}(\mathbf{x}, \hat{\mathbf{x}}) + p_G(\mathbf{x}, \hat{\mathbf{x}})} \quad (9)$$

The proofs of all theoretical results in this paper (including the following) are deferred in Appendix A.

**Theorem 1.** *Assume that  $\omega^+ = -\omega^- = c$  is constant, under the optimal self-supervised discriminator  $\hat{D}^*$ , optimizing the self-supervised task for the generator  $G$  is equivalent to:*

$$\min_G 4c \cdot M_{\text{AH}}(p_{\text{data}}(\mathbf{x}, \hat{\mathbf{x}}) \| p_G(\mathbf{x}, \hat{\mathbf{x}})), \quad (10)$$

where  $c = \|c\|_2^2$  is constant and  $M_{\text{AH}}$  is the arithmetic–harmonic mean (AHM) divergence [35], of which minimum is achieved if and only if  $p_G(\mathbf{x}, \hat{\mathbf{x}}) = p_{\text{data}}(\mathbf{x}, \hat{\mathbf{x}}) \Rightarrow p_G(\mathbf{x}) = p_{\text{data}}(\mathbf{x})$ .

Theorem 1 reveals that the generator of AugSelf-GAN theoretically still satisfies generative modeling, i.e., accurately learning the target data distribution, under certain assumptions. Although AugSelf-GAN does not obey the strict assumption, we note that this is not rare in the literature.<sup>2</sup> Under this assumption, AugSelf-GAN can be regarded as a multi-dimensional extension of the LS-GAN [27] in terms of the loss function, while excluding that of the generator. Additionally, our analysis offers an alternative theoretically grounded generator loss function for the LS-GAN family.<sup>3</sup>

**Corollary 1.** *The following equality and inequality hold for the AHM divergence:*

- $M_{\text{AH}}(p_{\text{data}}(\mathbf{x}, \hat{\mathbf{x}}) \| p_G(\mathbf{x}, \hat{\mathbf{x}})) + M_{\text{AH}}(p_G(\mathbf{x}, \hat{\mathbf{x}}) \| p_{\text{data}}(\mathbf{x}, \hat{\mathbf{x}})) = \Delta(p_{\text{data}}(\mathbf{x}, \hat{\mathbf{x}}) \| p_G(\mathbf{x}, \hat{\mathbf{x}}))$
- $M_{\text{AH}}(p_{\text{data}}(\mathbf{x}, \hat{\mathbf{x}}) \| p_G(\mathbf{x}, \hat{\mathbf{x}})) = 1 - W(p_{\text{data}}(\mathbf{x}, \hat{\mathbf{x}}) \| p_G(\mathbf{x}, \hat{\mathbf{x}})) \leq 1$

where  $\Delta$  is the Le Cam (LC) divergence [22], and  $W$  is the harmonic mean divergence [35].

Corollary 1 reveals a inequality  $M_{\text{AH}}(p_{\text{data}}(\mathbf{x}, \hat{\mathbf{x}}) \| p_G(\mathbf{x}, \hat{\mathbf{x}})) \leq \Delta(p_{\text{data}}(\mathbf{x}, \hat{\mathbf{x}}) \| p_G(\mathbf{x}, \hat{\mathbf{x}}))$  because of non-negativity of AHM divergence  $M_{\text{AH}}(p_G(\mathbf{x}, \hat{\mathbf{x}}) \| p_{\text{data}}(\mathbf{x}, \hat{\mathbf{x}})) \geq 0$ . Figure 4 plots the function  $f$  in AHM divergence and other common  $f$ -divergences used in the GAN literature. The AHM divergence shows better robustness of function  $f$  than others for extremely large inputs  $p(\mathbf{x})/q(\mathbf{x}) = D^*(\mathbf{x})/(1 - D^*(\mathbf{x}))$ , which is likely for the optimal discriminator  $D^*$  in data-limited scenarios.

<sup>2</sup>[9] analyzed that saturated GAN optimize Jensen Shannon (JS) divergence, but in fact it uses non-saturated loss, and LeCam-GAN [38] showed a connection between the Le Cam (LC) divergence [22] and its objective function based on fixed regularization, but in practice they use exponential moving average.

<sup>3</sup>The theoretical analysis of LS-GAN is actually inconsistent with its generator loss function.

Table 1: IS and FID comparisons of AugSelf-BigGAN with state-of-the-art methods on CIFAR-10 and CIFAR-100 with full and limited data. The best result is **bold** and the second best is underlined.

	Method	100% training data		20% training data		10% training data	
		IS ( $\uparrow$ )	FID ( $\downarrow$ )	IS ( $\uparrow$ )	FID ( $\downarrow$ )	IS ( $\uparrow$ )	FID ( $\downarrow$ )
CIFAR-10	BigGAN [2]	9.07	9.59	8.52	21.58	7.09	39.78
	DiffAugment [45]	9.16	8.70	8.65	14.04	8.09	22.40
	CR-GAN [44]	9.17	8.49	8.61	12.84	8.49	18.70
	LeCam-GAN [38]	<b>9.43</b>	8.28	8.83	12.56	8.57	17.68
	DigGAN [7]	<u>9.28</u>	8.49	8.89	13.01	8.32	17.87
	Tickets [3]	-	8.19	-	12.83	-	16.74
	MaskedGAN [13]	-	8.41 $\pm$ .03	-	12.51 $\pm$ .09	-	15.89 $\pm$ .12
	GenCo [6]	-	7.98 $\pm$ .02	-	12.61 $\pm$ .05	-	18.10 $\pm$ .06
	AugSelf-BigGAN	<b>9.43<math>\pm</math>.14</b>	7.68 $\pm$ .06	8.98 $\pm$ .09	<u>10.97<math>\pm</math>.09</u>	8.76 $\pm$ .05	<u>15.68<math>\pm</math>.26</u>
	AugSelf-BigGAN+	9.27 $\pm$ .05	<b>7.54<math>\pm</math>.04</b>	<b>9.08<math>\pm</math>.04</b>	<b>9.95<math>\pm</math>.17</b>	<b>8.79<math>\pm</math>.04</b>	<b>12.76<math>\pm</math>.14</b>
CIFAR-100	BigGAN [2]	10.71	12.87	8.58	33.11	6.74	66.71
	DiffAugment [45]	10.66	12.00	9.47	22.14	8.38	33.70
	CR-GAN [44]	10.81	11.25	9.12	20.28	8.70	26.90
	LeCam-GAN [38]	11.05	11.20	9.81	18.03	9.27	27.63
	DigGAN [7]	<b>11.45</b>	11.63	9.54	19.79	8.98	24.59
	Tickets [3]	-	10.73	-	17.43	-	23.80
	MaskedGAN [13]	-	11.65 $\pm$ .03	-	18.33 $\pm$ .09	-	24.02 $\pm$ .12
	GenCo [6]	-	10.92 $\pm$ .02	-	18.44 $\pm$ .04	-	25.22 $\pm$ .06
	AugSelf-BigGAN	<u>11.19<math>\pm</math>.09</u>	<b>9.88<math>\pm</math>.07</b>	<b>10.25<math>\pm</math>.06</b>	<u>16.11<math>\pm</math>.25</u>	<u>9.78<math>\pm</math>.08</u>	<u>21.30<math>\pm</math>.15</u>
	AugSelf-BigGAN+	11.12 $\pm$ .10	<u>10.09<math>\pm</math>.05</u>	<u>10.14<math>\pm</math>.11</u>	<b>15.33<math>\pm</math>.20</b>	<b>9.93<math>\pm</math>.06</b>	<b>18.64<math>\pm</math>.09</b>

Table 2: FID comparison of AugSelf-StyleGAN2 with competing methods on FFHQ and LSUN-Cat with limited training samples. The best result is **bold** and the second best is underlined.

Method	FFHQ				LSUN-Cat			
	30K	10K	5K	1K	30K	10K	5K	1K
StyleGAN2 [19]	6.16	14.75	26.60	62.16	10.12	17.93	34.69	182.85
+ ADA [16]	5.46	8.13	10.96	<u>21.29</u>	10.50	13.13	16.95	43.25
+ DiffAugment [45]	5.05	7.86	10.45	25.66	9.68	12.07	16.11	42.26
AugSelf-StyleGAN2	<b>4.95</b>	6.98	9.69	23.38	<b>9.22</b>	<b>11.98</b>	14.86	36.76
AugSelf-StyleGAN2+	5.82	<b>6.65</b>	<b>9.15</b>	<b>20.39</b>	<u>9.43</u>	<u>12.00</u>	<b>14.12</b>	<b>26.52</b>

## 6 Experiments

We implement AugSelf-GAN based on DiffAugment [45], keeping the network architectures and training settings unchanged for a fair comparison with prior work. Two common evaluation metrics, IS [32] and FID [10], are used to measure the generation performance. The mean and standard deviation (if reported) are obtained with five evaluation runs using the best FID checkpoint.

### 6.1 Comparison with State-of-the-Art Methods

**CIFAR-10 and CIFAR-100** Table 1 reports the results on CIFAR-10 and CIFAR-100 [20]. These experiments are based on the BigGAN architecture [2]. Our method significantly outperforms the direct baseline DiffAugment [45] and yields the best generation performance in terms of FID and IS compared with state-of-the-art methods. Notably, our method achieves further improvements when using stronger augmentation (AugSelf-BigGAN+ (translation $\uparrow$  and cutout $\uparrow$ ), see Table 5).

**FFHQ and LSUN-Cat** Table 2 reports the FID results on FFHQ [18] and LSUN-Cat [43]. The hyper-parameter is  $\lambda_g = 0.2$ . AugSelf-GAN performs substantially better than baselines with the same network backbone. Also, stronger augmentation (AugSelf-StyleGAN2+ (translation $\uparrow$  and cutout $\uparrow$ )) further improves the performance when training data is very limited.

Table 3: FID comparison of AugSelf-StyleGAN2 with state-of-the-art methods with and without pre-training on five low-shot datasets. The best result is **bold** and the second best is underlined.

Method	Pre-training?	100-shot			AnimalFaces	
		Obama	Grumpy cat	Panda	Cat	Dog
Scale/shift [29]	Yes	50.72	34.20	21.38	54.83	83.04
MineGAN [39]	Yes	50.63	34.54	14.84	54.45	93.03
TransferGAN [40]	Yes	48.73	34.06	23.20	52.61	82.38
FreezeD [28]	Yes	<u>41.87</u>	31.22	17.95	47.70	70.46
StyleGAN2 [19]	No	80.20	48.90	34.27	71.71	130.19
+ AdvAug [3]	No	52.86	31.02	14.75	47.40	68.28
+ ADA [16]	No	45.69	<u>26.62</u>	12.90	<u>40.77</u>	<u>56.83</u>
+ APA [15]	No	42.97	28.10	19.21	42.60	81.16
+ DiffAugment [45]	No	46.87	27.08	<u>12.06</u>	42.44	58.85
AugSelf-StyleGAN2	No	<b>26.00</b>	<b>19.81</b>	<b>8.36</b>	<b>30.53</b>	<b>48.19</b>

Table 4: FID comparison with fixed self-supervision ( $\omega^+ = -\omega^- = 1$ ). The best result is **bold**.

Method		100% training data		20% training data		10% training data	
		IS ( $\uparrow$ )	FID ( $\downarrow$ )	IS ( $\uparrow$ )	FID ( $\downarrow$ )	IS ( $\uparrow$ )	FID ( $\downarrow$ )
CIFAR-10	Fixed ( $c = 1$ )	9.25 $\pm$ .17	8.01 $\pm$ .05	8.70 $\pm$ .12	12.58 $\pm$ .16	8.53 $\pm$ .05	17.66 $\pm$ .55
	AugSelf-GAN	<b>9.43</b> $\pm$ .14	<b>7.68</b> $\pm$ .06	<b>8.98</b> $\pm$ .09	<b>10.97</b> $\pm$ .09	<b>8.76</b> $\pm$ .05	<b>15.68</b> $\pm$ .26
CIFAR-100	Fixed ( $c = 1$ )	10.67 $\pm$ .06	12.02 $\pm$ .07	9.94 $\pm$ .06	17.70 $\pm$ .17	9.50 $\pm$ .13	22.84 $\pm$ .28
	AugSelf-GAN	<b>11.19</b> $\pm$ .09	<b>9.88</b> $\pm$ .07	<b>10.25</b> $\pm$ .06	<b>16.11</b> $\pm$ .25	<b>9.78</b> $\pm$ .08	<b>21.30</b> $\pm$ .15

**Low-Shot Datasets** Table 3 shows the FID results on five common low-shot datasets [34] (Obama, Grumpy cat, Panda, and AnimalFace cat, and AnimalFace dog). The baselines are divided into two categories according to whether they were pre-trained. Due to its training stability, we are allowed to train AugSelf-StyleGAN2 for 5k generator update steps to ensure convergence. The hyper-parameters are  $\lambda_d = \lambda_g = 0.1$  on Grumpy cat and AnimalFace cat, and the self-supervision is color on all datasets. Impressively, AugSelf-StyleGAN2 surpasses competing methods by a large margin on all low-shot datasets, achieving new SOTA FID. More visual results are referred to Appendix D.

## 6.2 Analysis of AugSelf-GAN

**Fixed Supervision** Table 4 reports the results of AugSelf-GAN on CIFAR-10 and CIFAR-100 compared to the setup using fixed self-supervision, i.e.,  $\omega^+ = -\omega^- = 1$ , which corresponds to the assumption in Theorem 1. AugSelf-GAN outperforms the fixed setup in terms of both IS and FID in all training data regimes. The reason is somewhat intuitive, as a fixed self-supervision cannot enable the discriminator to learn semantic information related to data augmentation.

**Stronger Augmentation** Translation and cutout actually erase parts of image information, which help prevent the discriminator from overfitting, but could suffer from underfitting if excessive. Our self-supervised task enables the discriminator to be aware of different levels of translation and cutout, which helps alleviate underfitting and allows us to explore stronger translation and cutout. Table 5 compares AugSelf-GAN with DiffAugment in this setting. Overall, when data is limited, AugSelf-GAN can further benefit from stronger translation and cutout, while DiffAugment cannot.

**Hyper-parameters** Figure 5 plots the FID results of AugSelf-GAN with different hyper-parameters  $\lambda = \lambda_d = \lambda_g$  ranging from  $[0, 10]$  on CIFAR-10 and CIFAR-100. Notice that  $\lambda = 0$  corresponds to the baseline BigGAN + DiffAugment. AugSelf-BigGAN performs the best when  $\lambda$  is near 1. It is worth noting that AugSelf-BigGAN outperforms the baseline even for  $\lambda = 10$  with 10% and 20% training data, demonstrating superior robustness with respect to the coefficient hyper-parameter  $\lambda$ .

Table 5: Study on stronger augmentation. The best is **bold** and the second best is underlined.

	Method	100% training data		20% training data		10% training data	
		IS ( $\uparrow$ )	FID ( $\downarrow$ )	IS ( $\uparrow$ )	FID ( $\downarrow$ )	IS ( $\uparrow$ )	FID ( $\downarrow$ )
CIFAR-10	DiffAugment	9.29 $\pm$ .02	8.48 $\pm$ .13	8.84 $\pm$ .12	15.14 $\pm$ .47	<b>8.80</b> $\pm$ .01	20.60 $\pm$ .13
	+ translation $\uparrow$	9.21 $\pm$ .07	8.28 $\pm$ .17	8.88 $\pm$ .07	14.50 $\pm$ .23	8.61 $\pm$ .13	21.66 $\pm$ .21
	+ trans. $\uparrow$ cut. $\uparrow$	9.28 $\pm$ .06	8.42 $\pm$ .18	8.78 $\pm$ .06	14.28 $\pm$ .27	8.69 $\pm$ .07	20.93 $\pm$ .21
	AugSelf-GAN	<b>9.43</b> $\pm$ .14	7.68 $\pm$ .06	8.98 $\pm$ .09	10.97 $\pm$ .09	8.76 $\pm$ .05	15.68 $\pm$ .26
	+ translation $\uparrow$	<u>9.34</u> $\pm$ .07	<b>7.42</b> $\pm$ .09	8.98 $\pm$ .09	<u>10.45</u> $\pm$ .17	<u>8.79</u> $\pm$ .02	<u>14.64</u> $\pm$ .28
	+ trans. $\uparrow$ cut. $\uparrow$	9.27 $\pm$ .05	<u>7.54</u> $\pm$ .04	<b>9.08</b> $\pm$ .04	<b>9.95</b> $\pm$ .17	<u>8.79</u> $\pm$ .04	<b>12.76</b> $\pm$ .14
CIFAR-100	DiffAugment	11.02 $\pm$ .07	11.49 $\pm$ .21	9.45 $\pm$ .05	24.98 $\pm$ .48	8.50 $\pm$ .09	34.92 $\pm$ .63
	+ translation $\uparrow$	10.88 $\pm$ .10	11.61 $\pm$ .40	9.66 $\pm$ .10	23.63 $\pm$ .40	8.73 $\pm$ .04	35.15 $\pm$ .32
	+ trans. $\uparrow$ cut. $\uparrow$	11.10 $\pm$ .08	11.28 $\pm$ .20	9.58 $\pm$ .05	24.10 $\pm$ .66	8.59 $\pm$ .04	35.32 $\pm$ .46
	AugSelf-GAN	<u>11.19</u> $\pm$ .09	<u>9.88</u> $\pm$ .07	<b>10.25</b> $\pm$ .06	16.11 $\pm$ .25	9.78 $\pm$ .08	21.30 $\pm$ .15
	+ translation $\uparrow$	<b>11.22</b> $\pm$ .07	<b>9.63</b> $\pm$ .12	10.06 $\pm$ .10	<u>15.96</u> $\pm$ .26	<b>10.01</b> $\pm$ .12	<u>19.88</u> $\pm$ .20
	+ trans. $\uparrow$ cut. $\uparrow$	11.12 $\pm$ .10	10.09 $\pm$ .05	<u>10.14</u> $\pm$ .11	<b>15.33</b> $\pm$ .20	<u>9.93</u> $\pm$ .06	<b>18.64</b> $\pm$ .09

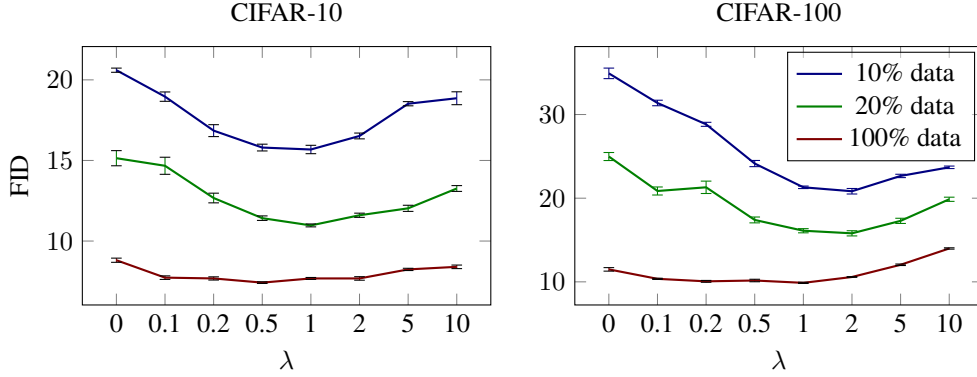


Figure 5: FID curves with varying hyper-parameters  $\lambda = \lambda_d = \lambda_g \in [0, 10]$  on CIFAR-10 and CIFAR-100. The hyper-parameter  $\lambda = 0$  corresponds to the baseline BigGAN + DiffAugment.

## 7 Conclusion

This paper proposes a data-efficient GAN training method by utilizing the augmentation parameter as self-supervision. Specifically, in addition to the original real-vs-fake task, the discriminator is also required to predict the augmentation parameter of the augmented data as well as the realness, forming a new augmentation-aware self-supervised discriminator, and the generator is encouraged to produce augmentation-predictable real but not fake data. Theoretical analysis reveals a connection between the optimization objective of the generator and the arithmetic–harmonic mean divergence. Experiments on data-limited benchmarks demonstrate the superior performance of the method compared to state-of-the-art methods, and extensive studies thoroughly verify each design of the method.

**Limitations** In our experiments, we observed that the improvements of AugSelf-GAN might be less pronounced under sufficient training data. Furthermore, its effectiveness depends on the specific data augmentation used. In some cases, inappropriate data augmentation may limit the improvements. Therefore, exploring advanced data augmentation can serve as future work.

**Broader Impacts** This work aims at improving GANs under limited training data. While this may result in negative societal impacts, such as lowering the threshold of generating fake content or exacerbating bias and discrimination due to data issues, we believe that these risks can be mitigated. By establishing ethical guidelines for users and exploring fake content detection techniques, one can prevent these undesirable outcomes. Furthermore, this work contributes to the overall development of GANs and even generative models, ultimately promoting their potential benefits for society.

## References

- [1] G. Baykal, F. Ozcelik, and G. Unal. Exploring deshuffle-gans in self-supervised generative adversarial networks. *Pattern Recognition*, 122:108244, 2022.
- [2] A. Brock, J. Donahue, and K. Simonyan. Large scale GAN training for high fidelity natural image synthesis. In *International Conference on Learning Representations*, 2019.
- [3] T. Chen, Y. Cheng, Z. Gan, J. Liu, and Z. Wang. Data-efficient gan training beyond (just) augmentations: A lottery ticket perspective. In M. Ranzato, A. Beygelzimer, Y. Dauphin, P. Liang, and J. W. Vaughan, editors, *Advances in Neural Information Processing Systems*, volume 34, pages 20941–20955. Curran Associates, Inc., 2021.
- [4] T. Chen, X. Zhai, M. Ritter, M. Lucic, and N. Houlsby. Self-supervised gans via auxiliary rotation loss. In *Proceedings of the IEEE/CVF Conference on Computer Vision and Pattern Recognition (CVPR)*, June 2019.
- [5] X. Chen, Z. Zhang, Y. Sui, and T. Chen. {GAN}s can play lottery tickets too. In *International Conference on Learning Representations*, 2021.
- [6] K. Cui, J. Huang, Z. Luo, G. Zhang, F. Zhan, and S. Lu. Genco: Generative co-training for generative adversarial networks with limited data. *Proceedings of the AAAI Conference on Artificial Intelligence*, 36(1):499–507, Jun. 2022.
- [7] T. Fang, R. Sun, and A. Schwing. Diggan: Discriminator gradient gap regularization for gan training with limited data. In S. Koyejo, S. Mohamed, A. Agarwal, D. Belgrave, K. Cho, and A. Oh, editors, *Advances in Neural Information Processing Systems*, volume 35, pages 31782–31795. Curran Associates, Inc., 2022.
- [8] S. Gidaris, P. Singh, and N. Komodakis. Unsupervised representation learning by predicting image rotations. In *International Conference on Learning Representations*, 2018.
- [9] I. Goodfellow, J. Pouget-Abadie, M. Mirza, B. Xu, D. Warde-Farley, S. Ozair, A. Courville, and Y. Bengio. Generative adversarial nets. In Z. Ghahramani, M. Welling, C. Cortes, N. Lawrence, and K. Weinberger, editors, *Advances in Neural Information Processing Systems*, volume 27. Curran Associates, Inc., 2014.
- [10] M. Heusel, H. Ramsauer, T. Unterthiner, B. Nessler, and S. Hochreiter. Gans trained by a two time-scale update rule converge to a local nash equilibrium. In I. Guyon, U. V. Luxburg, S. Bengio, H. Wallach, R. Fergus, S. Vishwanathan, and R. Garnett, editors, *Advances in Neural Information Processing Systems*, volume 30. Curran Associates, Inc., 2017.
- [11] L. Hou, Q. Cao, H. Shen, S. Pan, X. Li, and X. Cheng. Conditional GANs with auxiliary discriminative classifier. In K. Chaudhuri, S. Jegelka, L. Song, C. Szepesvari, G. Niu, and S. Sabato, editors, *Proceedings of the 39th International Conference on Machine Learning*, volume 162 of *Proceedings of Machine Learning Research*, pages 8888–8902. PMLR, 17–23 Jul 2022.
- [12] L. Hou, H. Shen, Q. Cao, and X. Cheng. Self-supervised gans with label augmentation. In M. Ranzato, A. Beygelzimer, Y. Dauphin, P. Liang, and J. W. Vaughan, editors, *Advances in Neural Information Processing Systems*, volume 34, pages 13019–13031. Curran Associates, Inc., 2021.
- [13] J. Huang, K. Cui, D. Guan, A. Xiao, F. Zhan, S. Lu, S. Liao, and E. Xing. Masked generative adversarial networks are data-efficient generation learners. In S. Koyejo, S. Mohamed, A. Agarwal, D. Belgrave, K. Cho, and A. Oh, editors, *Advances in Neural Information Processing Systems*, volume 35, pages 2154–2167. Curran Associates, Inc., 2022.
- [14] J. Jeong and J. Shin. Training {gan}s with stronger augmentations via contrastive discriminator. In *International Conference on Learning Representations*, 2021.
- [15] L. Jiang, B. Dai, W. Wu, and C. C. Loy. Deceive d: Adaptive pseudo augmentation for gan training with limited data. In M. Ranzato, A. Beygelzimer, Y. Dauphin, P. Liang, and J. W. Vaughan, editors, *Advances in Neural Information Processing Systems*, volume 34, pages 21655–21667. Curran Associates, Inc., 2021.

- [16] T. Karras, M. Aittala, J. Hellsten, S. Laine, J. Lehtinen, and T. Aila. Training generative adversarial networks with limited data. In H. Larochelle, M. Ranzato, R. Hadsell, M. Balcan, and H. Lin, editors, *Advances in Neural Information Processing Systems*, volume 33, pages 12104–12114. Curran Associates, Inc., 2020.
- [17] T. Karras, M. Aittala, S. Laine, E. Härkönen, J. Hellsten, J. Lehtinen, and T. Aila. Alias-free generative adversarial networks. In M. Ranzato, A. Beygelzimer, Y. Dauphin, P. Liang, and J. W. Vaughan, editors, *Advances in Neural Information Processing Systems*, volume 34, pages 852–863. Curran Associates, Inc., 2021.
- [18] T. Karras, S. Laine, and T. Aila. A style-based generator architecture for generative adversarial networks. In *Proceedings of the IEEE/CVF Conference on Computer Vision and Pattern Recognition (CVPR)*, June 2019.
- [19] T. Karras, S. Laine, M. Aittala, J. Hellsten, J. Lehtinen, and T. Aila. Analyzing and improving the image quality of stylegan. In *Proceedings of the IEEE/CVF Conference on Computer Vision and Pattern Recognition (CVPR)*, June 2020.
- [20] A. Krizhevsky, G. Hinton, et al. Learning multiple layers of features from tiny images. 2009.
- [21] N. Kumari, R. Zhang, E. Shechtman, and J.-Y. Zhu. Ensembling off-the-shelf models for gan training. In *Proceedings of the IEEE/CVF Conference on Computer Vision and Pattern Recognition (CVPR)*, pages 10651–10662, June 2022.
- [22] L. Le Cam. *Asymptotic methods in statistical decision theory*. Springer Science & Business Media, 2012.
- [23] H. Lee, K. Lee, K. Lee, H. Lee, and J. Shin. Improving transferability of representations via augmentation-aware self-supervision. In M. Ranzato, A. Beygelzimer, Y. Dauphin, P. Liang, and J. W. Vaughan, editors, *Advances in Neural Information Processing Systems*, volume 34, pages 17710–17722. Curran Associates, Inc., 2021.
- [24] K. S. Lee, N.-T. Tran, and N.-M. Cheung. Infomax-gan: Improved adversarial image generation via information maximization and contrastive learning. In *Proceedings of the IEEE/CVF Winter Conference on Applications of Computer Vision (WACV)*, pages 3942–3952, January 2021.
- [25] J. H. Lim and J. C. Ye. Geometric gan. *arXiv preprint arXiv:1705.02894*, 2017.
- [26] B. Liu, Y. Zhu, K. Song, and A. Elgammal. Towards faster and stabilized {gan} training for high-fidelity few-shot image synthesis. In *International Conference on Learning Representations*, 2021.
- [27] X. Mao, Q. Li, H. Xie, R. Y. Lau, Z. Wang, and S. Paul Smolley. Least squares generative adversarial networks. In *Proceedings of the IEEE International Conference on Computer Vision (ICCV)*, Oct 2017.
- [28] S. Mo, M. Cho, and J. Shin. Freeze the discriminator: a simple baseline for fine-tuning gans. *arXiv preprint arXiv:2002.10964*, 2020.
- [29] A. Noguchi and T. Harada. Image generation from small datasets via batch statistics adaptation. In *Proceedings of the IEEE/CVF International Conference on Computer Vision (ICCV)*, October 2019.
- [30] S. Nowozin, B. Cseke, and R. Tomioka. f-gan: Training generative neural samplers using variational divergence minimization. In D. Lee, M. Sugiyama, U. Luxburg, I. Guyon, and R. Garnett, editors, *Advances in Neural Information Processing Systems*, volume 29. Curran Associates, Inc., 2016.
- [31] P. Patel, N. Kumari, M. Singh, and B. Krishnamurthy. Lt-gan: Self-supervised gan with latent transformation detection. In *Proceedings of the IEEE/CVF Winter Conference on Applications of Computer Vision (WACV)*, pages 3189–3198, January 2021.



- [32] T. Salimans, I. Goodfellow, W. Zaremba, V. Cheung, A. Radford, X. Chen, and X. Chen. Improved techniques for training gans. In D. Lee, M. Sugiyama, U. Luxburg, I. Guyon, and R. Garnett, editors, *Advances in Neural Information Processing Systems*, volume 29. Curran Associates, Inc., 2016.
- [33] A. Sauer, K. Chitta, J. Müller, and A. Geiger. Projected gans converge faster. In M. Ranzato, A. Beygelzimer, Y. Dauphin, P. Liang, and J. W. Vaughan, editors, *Advances in Neural Information Processing Systems*, volume 34, pages 17480–17492. Curran Associates, Inc., 2021.
- [34] Z. Si and S.-C. Zhu. Learning hybrid image templates (hit) by information projection. *IEEE Transactions on pattern analysis and machine intelligence*, 34(7):1354–1367, 2011.
- [35] I. J. Taneja. On mean divergence measures. *Advances in Inequalities from probability theory and statistics. Nova, USA*, pages 169–186, 2008.
- [36] N.-T. Tran, V.-H. Tran, B.-N. Nguyen, L. Yang, and N.-M. M. Cheung. Self-supervised gan: Analysis and improvement with multi-class minimax game. In H. Wallach, H. Larochelle, A. Beygelzimer, F. d'Alché-Buc, E. Fox, and R. Garnett, editors, *Advances in Neural Information Processing Systems*, volume 32. Curran Associates, Inc., 2019.
- [37] N.-T. Tran, V.-H. Tran, N.-B. Nguyen, T.-K. Nguyen, and N.-M. Cheung. On data augmentation for gan training. *IEEE Transactions on Image Processing*, 30:1882–1897, 2021.
- [38] H.-Y. Tseng, L. Jiang, C. Liu, M.-H. Yang, and W. Yang. Regularizing generative adversarial networks under limited data. In *Proceedings of the IEEE/CVF Conference on Computer Vision and Pattern Recognition (CVPR)*, pages 7921–7931, June 2021.
- [39] Y. Wang, A. Gonzalez-Garcia, D. Berga, L. Herranz, F. S. Khan, and J. v. d. Weijer. Minegan: Effective knowledge transfer from gans to target domains with few images. In *Proceedings of the IEEE/CVF Conference on Computer Vision and Pattern Recognition (CVPR)*, June 2020.
- [40] Y. Wang, C. Wu, L. Herranz, J. van de Weijer, A. Gonzalez-Garcia, and B. Raducanu. Transferring gans: generating images from limited data. In *Proceedings of the European Conference on Computer Vision (ECCV)*, September 2018.
- [41] C. Yang, Y. Shen, Y. Xu, and B. Zhou. Data-efficient instance generation from instance discrimination. In M. Ranzato, A. Beygelzimer, Y. Dauphin, P. Liang, and J. W. Vaughan, editors, *Advances in Neural Information Processing Systems*, volume 34, pages 9378–9390. Curran Associates, Inc., 2021.
- [42] m. yang, Z. Wang, Z. Chi, and Y. Zhang. Fregan: Exploiting frequency components for training gans under limited data. In S. Koyejo, S. Mohamed, A. Agarwal, D. Belgrave, K. Cho, and A. Oh, editors, *Advances in Neural Information Processing Systems*, volume 35, pages 33387–33399. Curran Associates, Inc., 2022.
- [43] F. Yu, A. Seff, Y. Zhang, S. Song, T. Funkhouser, and J. Xiao. Lsun: Construction of a large-scale image dataset using deep learning with humans in the loop. *arXiv preprint arXiv:1506.03365*, 2015.
- [44] H. Zhang, Z. Zhang, A. Odena, and H. Lee. Consistency regularization for generative adversarial networks. In *International Conference on Learning Representations*, 2020.
- [45] S. Zhao, Z. Liu, J. Lin, J.-Y. Zhu, and S. Han. Differentiable augmentation for data-efficient gan training. In H. Larochelle, M. Ranzato, R. Hadsell, M. Balcan, and H. Lin, editors, *Advances in Neural Information Processing Systems*, volume 33, pages 7559–7570. Curran Associates, Inc., 2020.
- [46] Z. Zhao, Z. Zhang, T. Chen, S. Singh, and H. Zhang. Image augmentations for gan training. *arXiv preprint arXiv:2006.02595*, 2020.

## A Proofs

**Proposition 1.** For any generator  $G$  and given unlimited capacity in the function space, the optimal augmentation-aware self-supervised discriminator  $\hat{D}^*$  has the form of:

$$\hat{D}^*(\hat{\mathbf{x}}, \mathbf{x}) = \frac{\int p_{\text{data}}(\mathbf{x}, \boldsymbol{\omega}, \hat{\mathbf{x}}) \boldsymbol{\omega}^+ d\boldsymbol{\omega} + \int p_G(\mathbf{x}, \boldsymbol{\omega}, \hat{\mathbf{x}}) \boldsymbol{\omega}^- d\boldsymbol{\omega}}{p_{\text{data}}(\mathbf{x}, \hat{\mathbf{x}}) + p_G(\mathbf{x}, \hat{\mathbf{x}})} \quad (9)$$

*Proof.* The objective function of the self-supervised discriminator can be written as follows:

$$\begin{aligned} \mathcal{L}_D^{\text{ss}} &= \mathbb{E}_{\mathbf{x}, \boldsymbol{\omega}} \left[ \|\hat{D}(T(\mathbf{x}; \boldsymbol{\omega}), \mathbf{x}) - \boldsymbol{\omega}^+\|_2^2 \right] + \mathbb{E}_{\mathbf{z}, \boldsymbol{\omega}} \left[ \|\hat{D}(T(G(\mathbf{z}); \boldsymbol{\omega}), G(\mathbf{z})) - \boldsymbol{\omega}^-\|_2^2 \right] \\ &= \iiint \left[ p_{\text{data}}(\mathbf{x}, \boldsymbol{\omega}, \hat{\mathbf{x}}) \|\hat{D}(\hat{\mathbf{x}}, \mathbf{x}) - \boldsymbol{\omega}^+\|_2^2 + p_G(\mathbf{x}, \boldsymbol{\omega}, \hat{\mathbf{x}}) \|\hat{D}(\hat{\mathbf{x}}, \mathbf{x}) - \boldsymbol{\omega}^-\|_2^2 \right] d\mathbf{x} d\boldsymbol{\omega} d\hat{\mathbf{x}} \end{aligned}$$

Minimizing the integral objective is equivalent to minimizing the objective on each data point:

$$\mathcal{L}_D^{\text{ss}}(\mathbf{x}, \hat{\mathbf{x}}) = \int \left[ p_{\text{data}}(\mathbf{x}, \boldsymbol{\omega}, \hat{\mathbf{x}}) \|\hat{D}(\hat{\mathbf{x}}, \mathbf{x}) - \boldsymbol{\omega}^+\|_2^2 + p_G(\mathbf{x}, \boldsymbol{\omega}, \hat{\mathbf{x}}) \|\hat{D}(\hat{\mathbf{x}}, \mathbf{x}) - \boldsymbol{\omega}^-\|_2^2 \right] d\boldsymbol{\omega}$$

Get its derivative with respect to the self-supervised discriminator and let it equals to 0, we have the optimal self-supervised discriminator as:

$$\begin{aligned} \frac{\partial \mathcal{L}_D^{\text{ss}}}{\partial \hat{D}(\hat{\mathbf{x}}, \mathbf{x})} &= \int \left[ p_{\text{data}}(\mathbf{x}, \boldsymbol{\omega}, \hat{\mathbf{x}}) 2(\hat{D}(\hat{\mathbf{x}}, \mathbf{x}) - \boldsymbol{\omega}^+) + p_G(\mathbf{x}, \boldsymbol{\omega}, \hat{\mathbf{x}}) 2(\hat{D}(\hat{\mathbf{x}}, \mathbf{x}) - \boldsymbol{\omega}^-) \right] d\boldsymbol{\omega} = 0 \\ \Rightarrow \hat{D}^*(\hat{\mathbf{x}}, \mathbf{x}) &= \frac{\int p_{\text{data}}(\mathbf{x}, \boldsymbol{\omega}, \hat{\mathbf{x}}) \boldsymbol{\omega}^+ d\boldsymbol{\omega} + \int p_G(\mathbf{x}, \boldsymbol{\omega}, \hat{\mathbf{x}}) \boldsymbol{\omega}^- d\boldsymbol{\omega}}{p_{\text{data}}(\mathbf{x}, \hat{\mathbf{x}}) + p_G(\mathbf{x}, \hat{\mathbf{x}})} \end{aligned}$$

□

**Theorem 1.** Assume that  $\boldsymbol{\omega}^+ = -\boldsymbol{\omega}^- = \mathbf{c}$  is constant, under the optimal self-supervised discriminator  $\hat{D}^*$ , optimizing the self-supervised task for the generator  $G$  is equivalent to:

$$\min_G 4c \cdot M_{\text{AH}}(p_{\text{data}}(\mathbf{x}, \hat{\mathbf{x}}) \| p_G(\mathbf{x}, \hat{\mathbf{x}})), \quad (10)$$

where  $c = \|\mathbf{c}\|_2^2$  is constant and  $M_{\text{AH}}$  is the arithmetic–harmonic mean (AHM) divergence [35], of which minimum is achieved if and only if  $p_G(\mathbf{x}, \hat{\mathbf{x}}) = p_{\text{data}}(\mathbf{x}, \hat{\mathbf{x}}) \Rightarrow p_G(\mathbf{x}) = p_{\text{data}}(\mathbf{x})$ .

*Proof.* The objective function of the self-supervised task for the generator can be written as follows:

$$\begin{aligned} &\mathbb{E}_{\mathbf{z}, \boldsymbol{\omega}} \left[ \|\hat{D}(T(G(\mathbf{z}); \boldsymbol{\omega}), G(\mathbf{z})) - \boldsymbol{\omega}^+\|_2^2 \right] - \mathbb{E}_{\mathbf{z}, \boldsymbol{\omega}} \left[ \|\hat{D}(T(G(\mathbf{z}); \boldsymbol{\omega}), G(\mathbf{z})) - \boldsymbol{\omega}^-\|_2^2 \right] \\ &= \iiint p_G(\mathbf{x}, \boldsymbol{\omega}, \hat{\mathbf{x}}) \left[ \|\hat{D}(\mathbf{x}, \hat{\mathbf{x}}) - \boldsymbol{\omega}^+\|_2^2 - \|\hat{D}(\mathbf{x}, \hat{\mathbf{x}}) - \boldsymbol{\omega}^-\|_2^2 \right] d\mathbf{x} d\boldsymbol{\omega} d\hat{\mathbf{x}} \\ &= \iint p_G(\mathbf{x}, \hat{\mathbf{x}}) \left[ \left\| \frac{\mathbf{c}(p_{\text{data}}(\mathbf{x}, \hat{\mathbf{x}}) - p_G(\mathbf{x}, \hat{\mathbf{x}}))}{p_{\text{data}}(\mathbf{x}, \hat{\mathbf{x}}) + p_G(\mathbf{x}, \hat{\mathbf{x}})} - \mathbf{c} \right\|_2^2 - \left\| \frac{\mathbf{c}(p_{\text{data}}(\mathbf{x}, \hat{\mathbf{x}}) - p_G(\mathbf{x}, \hat{\mathbf{x}}))}{p_{\text{data}}(\mathbf{x}, \hat{\mathbf{x}}) + p_G(\mathbf{x}, \hat{\mathbf{x}})} + \mathbf{c} \right\|_2^2 \right] d\mathbf{x} d\hat{\mathbf{x}} \\ &= c \cdot \iint p_G(\mathbf{x}, \hat{\mathbf{x}}) \left[ \left\| \frac{p_{\text{data}}(\mathbf{x}, \hat{\mathbf{x}}) - p_G(\mathbf{x}, \hat{\mathbf{x}})}{p_{\text{data}}(\mathbf{x}, \hat{\mathbf{x}}) + p_G(\mathbf{x}, \hat{\mathbf{x}})} - 1 \right\|_2^2 - \left\| \frac{p_{\text{data}}(\mathbf{x}, \hat{\mathbf{x}}) - p_G(\mathbf{x}, \hat{\mathbf{x}})}{p_{\text{data}}(\mathbf{x}, \hat{\mathbf{x}}) + p_G(\mathbf{x}, \hat{\mathbf{x}})} + 1 \right\|_2^2 \right] d\mathbf{x} d\hat{\mathbf{x}} \\ &= c \cdot \iint p_G(\mathbf{x}, \hat{\mathbf{x}}) \left[ \left\| \frac{2p_G(\mathbf{x}, \hat{\mathbf{x}})}{p_{\text{data}}(\mathbf{x}, \hat{\mathbf{x}}) + p_G(\mathbf{x}, \hat{\mathbf{x}})} \right\|_2^2 - \left\| \frac{2p_{\text{data}}(\mathbf{x}, \hat{\mathbf{x}})}{p_{\text{data}}(\mathbf{x}, \hat{\mathbf{x}}) + p_G(\mathbf{x}, \hat{\mathbf{x}})} \right\|_2^2 \right] d\mathbf{x} d\hat{\mathbf{x}} \\ &= 4c \cdot \iint p_G(\mathbf{x}, \hat{\mathbf{x}}) \left[ \frac{p_G(\mathbf{x}, \hat{\mathbf{x}})^2 - p_{\text{data}}(\mathbf{x}, \hat{\mathbf{x}})^2}{(p_{\text{data}}(\mathbf{x}, \hat{\mathbf{x}}) + p_G(\mathbf{x}, \hat{\mathbf{x}}))^2} \right] d\mathbf{x} d\hat{\mathbf{x}} \\ &= 4c \cdot \iint p_G(\mathbf{x}, \hat{\mathbf{x}}) \left[ \frac{p_G(\mathbf{x}, \hat{\mathbf{x}}) - p_{\text{data}}(\mathbf{x}, \hat{\mathbf{x}})}{p_{\text{data}}(\mathbf{x}, \hat{\mathbf{x}}) + p_G(\mathbf{x}, \hat{\mathbf{x}})} \right] d\mathbf{x} d\hat{\mathbf{x}} \\ &= 4c \cdot M_{\text{AH}}(p_{\text{data}}(\mathbf{x}, \hat{\mathbf{x}}) \| p_G(\mathbf{x}, \hat{\mathbf{x}})) \end{aligned}$$

where  $c = \|\mathbf{c}\|_2^2$  is a constant scalar for the constant vector  $\mathbf{c} = \boldsymbol{\omega}^+ = -\boldsymbol{\omega}^-$ . And we have the optimal generator  $p_G(\mathbf{x}, \hat{\mathbf{x}}) = p_{\text{data}}(\mathbf{x}, \hat{\mathbf{x}}) \Rightarrow p_G(\mathbf{x}) = p_{\text{data}}(\mathbf{x})$  to minimize the AHM divergence. □

**Corollary 1.** *The following equality and inequality hold for the AHM divergence:*

- $M_{\text{AH}}(p_{\text{data}}(\mathbf{x}, \hat{\mathbf{x}}) \| p_G(\mathbf{x}, \hat{\mathbf{x}})) + M_{\text{AH}}(p_G(\mathbf{x}, \hat{\mathbf{x}}) \| p_{\text{data}}(\mathbf{x}, \hat{\mathbf{x}})) = \Delta(p_{\text{data}}(\mathbf{x}, \hat{\mathbf{x}}) \| p_G(\mathbf{x}, \hat{\mathbf{x}}))$
- $M_{\text{AH}}(p_{\text{data}}(\mathbf{x}, \hat{\mathbf{x}}) \| p_G(\mathbf{x}, \hat{\mathbf{x}})) = 1 - W(p_{\text{data}}(\mathbf{x}, \hat{\mathbf{x}}) \| p_G(\mathbf{x}, \hat{\mathbf{x}})) \leq 1$

where  $\Delta$  is the Le Cam (LC) divergence [22], and  $W$  is the harmonic mean divergence [35].

*Proof.*

$$\begin{aligned}
& M_{\text{AH}}(p_{\text{data}}(\mathbf{x}, \hat{\mathbf{x}}) \| p_G(\mathbf{x}, \hat{\mathbf{x}})) \\
& \leq M_{\text{AH}}(p_{\text{data}}(\mathbf{x}, \hat{\mathbf{x}}) \| p_G(\mathbf{x}, \hat{\mathbf{x}})) + M_{\text{AH}}(p_G(\mathbf{x}, \hat{\mathbf{x}}) \| p_{\text{data}}(\mathbf{x}, \hat{\mathbf{x}})) \\
& = \iint p_G(\mathbf{x}, \hat{\mathbf{x}}) \frac{p_G(\mathbf{x}, \hat{\mathbf{x}}) - p_{\text{data}}(\mathbf{x}, \hat{\mathbf{x}})}{p_{\text{data}}(\mathbf{x}, \hat{\mathbf{x}}) + p_G(\mathbf{x}, \hat{\mathbf{x}})} d\mathbf{x} d\hat{\mathbf{x}} + \iint p_{\text{data}}(\mathbf{x}, \hat{\mathbf{x}}) \frac{p_{\text{data}}(\mathbf{x}, \hat{\mathbf{x}}) - p_G(\mathbf{x}, \hat{\mathbf{x}})}{p_G(\mathbf{x}, \hat{\mathbf{x}}) + p_{\text{data}}(\mathbf{x}, \hat{\mathbf{x}})} d\mathbf{x} d\hat{\mathbf{x}} \\
& = \iint p_G(\mathbf{x}, \hat{\mathbf{x}}) \frac{p_G(\mathbf{x}, \hat{\mathbf{x}}) - p_{\text{data}}(\mathbf{x}, \hat{\mathbf{x}})}{p_{\text{data}}(\mathbf{x}, \hat{\mathbf{x}}) + p_G(\mathbf{x}, \hat{\mathbf{x}})} d\mathbf{x} d\hat{\mathbf{x}} - \iint p_{\text{data}}(\mathbf{x}, \hat{\mathbf{x}}) \frac{p_G(\mathbf{x}, \hat{\mathbf{x}}) - p_{\text{data}}(\mathbf{x}, \hat{\mathbf{x}})}{p_G(\mathbf{x}, \hat{\mathbf{x}}) + p_{\text{data}}(\mathbf{x}, \hat{\mathbf{x}})} d\mathbf{x} d\hat{\mathbf{x}} \\
& = \iint \frac{(p_G(\mathbf{x}, \hat{\mathbf{x}}) - p_{\text{data}}(\mathbf{x}, \hat{\mathbf{x}}))^2}{p_{\text{data}}(\mathbf{x}, \hat{\mathbf{x}}) + p_G(\mathbf{x}, \hat{\mathbf{x}})} d\mathbf{x} d\hat{\mathbf{x}} \\
& = \Delta(p_{\text{data}}(\mathbf{x}, \hat{\mathbf{x}}) \| p_G(\mathbf{x}, \hat{\mathbf{x}}))
\end{aligned}$$

$$\begin{aligned}
0 & \leq M_{\text{AH}}(p_{\text{data}}(\mathbf{x}, \hat{\mathbf{x}}) \| p_G(\mathbf{x}, \hat{\mathbf{x}})) \\
& = \iint p_G(\mathbf{x}, \hat{\mathbf{x}}) \frac{p_G(\mathbf{x}, \hat{\mathbf{x}}) - p_{\text{data}}(\mathbf{x}, \hat{\mathbf{x}})}{p_{\text{data}}(\mathbf{x}, \hat{\mathbf{x}}) + p_G(\mathbf{x}, \hat{\mathbf{x}})} d\mathbf{x} d\hat{\mathbf{x}} \\
& = \iint p_G(\mathbf{x}, \hat{\mathbf{x}}) \left[ 1 - \frac{2p_{\text{data}}(\mathbf{x}, \hat{\mathbf{x}})}{p_{\text{data}}(\mathbf{x}, \hat{\mathbf{x}}) + p_G(\mathbf{x}, \hat{\mathbf{x}})} \right] d\mathbf{x} d\hat{\mathbf{x}} \\
& = 1 - \iint \frac{2p_{\text{data}}(\mathbf{x}, \hat{\mathbf{x}}) p_G(\mathbf{x}, \hat{\mathbf{x}})}{p_{\text{data}}(\mathbf{x}, \hat{\mathbf{x}}) + p_G(\mathbf{x}, \hat{\mathbf{x}})} d\mathbf{x} d\hat{\mathbf{x}} \\
& = 1 - W(p_{\text{data}}(\mathbf{x}, \hat{\mathbf{x}}) \| p_G(\mathbf{x}, \hat{\mathbf{x}})) \leq 1
\end{aligned}$$

where  $W(p_{\text{data}}(\mathbf{x}, \hat{\mathbf{x}}) \| p_G(\mathbf{x}, \hat{\mathbf{x}})) \geq 0$  is the well known harmonic mean divergence [35].  $\square$

## B Additional Results

**Self-Supervised Tasks** We introduce two non-adversarial self-supervised tasks for comparison. The first version is that the discriminator only learns self supervision on real data, defined as:

$$\mathcal{L}_D^{\text{ss}} = \mathbb{E}_{\mathbf{x} \sim p_{\text{data}}(\mathbf{x}), \omega \sim p(\omega)} \left[ \|\hat{D}(T(\mathbf{x}; \omega), \mathbf{x}) - \omega\|_2^2 \right]. \quad (11)$$

The second version is that the discriminator learns self supervised tasks on both real and generated data simultaneously, given by:

$$\mathcal{L}_D^{\text{ss}} = \mathbb{E}_{\mathbf{x}, \omega} \left[ \|\hat{D}(T(\mathbf{x}; \omega), \mathbf{x}) - \omega\|_2^2 \right] + \mathbb{E}_{\mathbf{z}, \omega} \left[ \|\hat{D}(T(G(\mathbf{z}); \omega), G(\mathbf{z})) - \omega\|_2^2 \right]. \quad (12)$$

For both versions, the generator is encouraged to produce augmentation-recognizable data, as follows:

$$\mathcal{L}_G^{\text{ss}} = \mathbb{E}_{\mathbf{z} \sim p(\mathbf{z}), \omega \sim p(\omega)} \left[ \|\hat{D}(T(G(\mathbf{z}); \omega), G(\mathbf{z})) - \omega\|_2^2 \right]. \quad (13)$$

According to the self-supervised task, we denote the methods as SS (Equations (11) and (13)), SS+ (Equations (12) and (13)), and ASS (Equations (5) and (6), short for adversarial self-supervised learning, i.e., the proposed AugSelf-GAN).

Table 6 reports the comparison between methods with different self-supervised tasks. We also conducted generator-free self-supervised learning experiments by setting the hyper-parameter as  $\lambda_g = 0$  on each kind of self supervised task. According to the FID score, ASS is significantly superior to SS and SS+. Even without the self supervised task of the generator, ASS ( $\lambda_g = 0$ ) outperforms SS and SS+ that include generator self supervised tasks in limited (10% and 20%) data, and the introduction of generator self supervised tasks further expands this advantage.

Table 6: IS and FID of AugSelf-BigGAN with different self-supervised tasks on CIFAR-10 and CIFAR-100 with full and limited training data. The best is **bold** and the second best is underlined.

Method	100% training data		20% training data		10% training data		
	IS ( $\uparrow$ )	FID ( $\downarrow$ )	IS ( $\uparrow$ )	FID ( $\downarrow$ )	IS ( $\uparrow$ )	FID ( $\downarrow$ )	
CIFAR-10	Baseline	9.29 $\pm$ 0.02	8.48 $\pm$ 0.13	8.84 $\pm$ 0.12	15.14 $\pm$ 0.47	<b>8.80</b> $\pm$ 0.01	20.60 $\pm$ 0.13
	SS ( $\lambda_g = 0$ )	9.28 $\pm$ 0.06	8.30 $\pm$ 0.12	8.86 $\pm$ 0.09	13.96 $\pm$ 0.19	8.62 $\pm$ 0.09	20.94 $\pm$ 0.42
	SS	<u>9.29</u> $\pm$ 0.07	8.24 $\pm$ 0.10	<b>8.98</b> $\pm$ 0.04	<u>13.42</u> $\pm$ 0.36	8.69 $\pm$ 0.05	19.40 $\pm$ 0.28
	SS+ ( $\lambda_g = 0$ )	9.25 $\pm$ 0.06	<u>8.11</u> $\pm$ 0.18	8.81 $\pm$ 0.05	13.86 $\pm$ 0.31	<u>8.76</u> $\pm$ 0.06	19.52 $\pm$ 0.24
	SS+	9.26 $\pm$ 0.04	8.26 $\pm$ 0.28	8.85 $\pm$ 0.05	13.81 $\pm$ 0.27	8.63 $\pm$ 0.05	19.85 $\pm$ 0.18
	ASS ( $\lambda_g = 0$ )	9.12 $\pm$ 0.05	8.90 $\pm$ 0.07	8.82 $\pm$ 0.03	13.65 $\pm$ 0.70	8.52 $\pm$ 0.04	<u>18.14</u> $\pm$ 0.33
	ASS	<b>9.43</b> $\pm$ 0.14	<b>7.68</b> $\pm$ 0.06	<b>8.98</b> $\pm$ 0.09	<b>10.97</b> $\pm$ 0.09	<u>8.76</u> $\pm$ 0.05	<b>15.68</b> $\pm$ 0.26
CIFAR-100	Baseline	11.02 $\pm$ 0.07	11.49 $\pm$ 0.21	9.45 $\pm$ 0.05	24.98 $\pm$ 0.48	8.50 $\pm$ 0.09	34.92 $\pm$ 0.63
	SS ( $\lambda_g = 0$ )	<u>11.04</u> $\pm$ 0.09	11.48 $\pm$ 0.43	9.81 $\pm$ 0.07	21.17 $\pm$ 0.19	9.11 $\pm$ 0.09	30.48 $\pm$ 0.57
	SS	10.96 $\pm$ 0.11	11.04 $\pm$ 0.15	<u>9.99</u> $\pm$ 0.09	20.72 $\pm$ 0.33	9.23 $\pm$ 0.07	31.54 $\pm$ 1.12
	SS+ ( $\lambda_g = 0$ )	10.84 $\pm$ 0.09	11.48 $\pm$ 0.13	9.95 $\pm$ 0.07	21.22 $\pm$ 0.57	9.14 $\pm$ 0.05	31.02 $\pm$ 1.00
	SS+	10.94 $\pm$ 0.10	<u>10.94</u> $\pm$ 0.12	9.88 $\pm$ 0.06	22.72 $\pm$ 0.37	9.23 $\pm$ 0.14	31.40 $\pm$ 0.22
	ASS ( $\lambda_g = 0$ )	10.82 $\pm$ 0.10	11.29 $\pm$ 0.12	9.96 $\pm$ 0.11	<u>18.90</u> $\pm$ 0.41	<u>9.45</u> $\pm$ 0.05	<u>25.77</u> $\pm$ 0.95
	ASS	<b>11.19</b> $\pm$ 0.09	<b>9.88</b> $\pm$ 0.07	<b>10.25</b> $\pm$ 0.06	<b>16.11</b> $\pm$ 0.25	<b>9.78</b> $\pm$ 0.08	<b>21.30</b> $\pm$ 0.15

Table 7: IS and FID of AugSelf-BigGAN with different self-supervised signals on CIFAR-10 and CIFAR-100 with full and limited training data. The self supervised signal to be predicted is marked by the symbol  $\checkmark$ . Notice that all methods adopt color, translation, and cutout as data augmentation.

	Self-Supervised Signals			100% training data		20% training data		10% training data	
	color	trans.	cutout	IS ( $\uparrow$ )	FID ( $\downarrow$ )	IS ( $\uparrow$ )	FID ( $\downarrow$ )	IS ( $\uparrow$ )	FID ( $\downarrow$ )
CIFAR-10	$\times$	$\times$	$\times$	9.29 $\pm$ 0.02	8.48 $\pm$ 0.13	8.84 $\pm$ 0.12	15.14 $\pm$ 0.47	8.80 $\pm$ 0.01	20.60 $\pm$ 0.13
	$\checkmark$	$\times$	$\times$	<b>9.50</b> $\pm$ 0.07	7.57 $\pm$ 0.07	<b>8.99</b> $\pm$ 0.06	11.38 $\pm$ 0.14	8.72 $\pm$ 0.09	16.50 $\pm$ 0.14
	$\times$	$\checkmark$	$\times$	9.39 $\pm$ 0.07	7.51 $\pm$ 0.12	8.95 $\pm$ 0.05	11.82 $\pm$ 0.21	8.80 $\pm$ 0.03	16.27 $\pm$ 0.35
	$\times$	$\times$	$\checkmark$	9.30 $\pm$ 0.05	7.48 $\pm$ 0.07	8.94 $\pm$ 0.07	11.73 $\pm$ 0.27	8.73 $\pm$ 0.12	16.66 $\pm$ 0.39
	$\checkmark$	$\checkmark$	$\times$	9.42 $\pm$ 0.06	7.43 $\pm$ 0.06	8.91 $\pm$ 0.09	11.19 $\pm$ 0.20	8.58 $\pm$ 0.02	<b>15.17</b> $\pm$ 0.15
	$\checkmark$	$\times$	$\checkmark$	9.41 $\pm$ 0.07	7.51 $\pm$ 0.05	8.92 $\pm$ 0.12	11.20 $\pm$ 0.17	<b>8.83</b> $\pm$ 0.07	15.55 $\pm$ 0.21
	$\times$	$\checkmark$	$\checkmark$	9.38 $\pm$ 0.05	<b>7.41</b> $\pm$ 0.11	8.87 $\pm$ 0.04	11.19 $\pm$ 0.08	8.63 $\pm$ 0.08	16.30 $\pm$ 0.57
	$\checkmark$	$\checkmark$	$\checkmark$	9.43 $\pm$ 0.14	7.68 $\pm$ 0.06	8.98 $\pm$ 0.09	<b>10.97</b> $\pm$ 0.09	8.76 $\pm$ 0.05	15.68 $\pm$ 0.26
CIFAR-100	$\times$	$\times$	$\times$	11.02 $\pm$ 0.07	11.49 $\pm$ 0.21	9.45 $\pm$ 0.05	24.98 $\pm$ 0.48	8.50 $\pm$ 0.09	34.92 $\pm$ 0.63
	$\checkmark$	$\times$	$\times$	11.20 $\pm$ 0.08	10.01 $\pm$ 0.13	9.90 $\pm$ 0.11	18.16 $\pm$ 0.62	9.39 $\pm$ 0.04	21.48 $\pm$ 0.14
	$\times$	$\checkmark$	$\times$	<b>11.35</b> $\pm$ 0.10	9.88 $\pm$ 0.08	10.01 $\pm$ 0.07	18.39 $\pm$ 0.07	9.29 $\pm$ 0.10	26.50 $\pm$ 0.36
	$\times$	$\times$	$\checkmark$	11.16 $\pm$ 0.13	10.03 $\pm$ 0.14	10.18 $\pm$ 0.09	19.45 $\pm$ 0.62	9.46 $\pm$ 0.12	25.99 $\pm$ 0.62
	$\checkmark$	$\checkmark$	$\times$	11.26 $\pm$ 0.16	<b>9.65</b> $\pm$ 0.04	10.21 $\pm$ 0.12	17.32 $\pm$ 0.51	9.92 $\pm$ 0.06	22.94 $\pm$ 0.17
	$\checkmark$	$\times$	$\checkmark$	11.17 $\pm$ 0.12	10.12 $\pm$ 0.20	10.14 $\pm$ 0.09	17.11 $\pm$ 0.62	<b>9.94</b> $\pm$ 0.12	24.52 $\pm$ 0.76
	$\times$	$\checkmark$	$\checkmark$	11.26 $\pm$ 0.07	9.75 $\pm$ 0.05	<b>10.35</b> $\pm$ 0.20	16.88 $\pm$ 0.46	9.92 $\pm$ 0.08	23.09 $\pm$ 0.72
	$\checkmark$	$\checkmark$	$\checkmark$	11.19 $\pm$ 0.09	9.88 $\pm$ 0.07	10.25 $\pm$ 0.06	<b>16.11</b> $\pm$ 0.25	9.78 $\pm$ 0.08	<b>21.30</b> $\pm$ 0.15

**Self-Supervised Signals** We empirically analyze the role of different augmentation parameters as self-supervised signals for AugSelf-GAN. All methods employ three types of data augmentations (color, translation, and cutout), with the difference lying in the predicted self-supervised signals. According to the FID scores in Table 7, predicting any augmentation parameters can significantly improve the final generative performance compared to the baseline. Although there is no significant difference among them, we still choose to predict all augmentation parameters as the default setting for AugSelf-GAN. This experiment demonstrates that the self-supervised task itself plays a decisive role in training data-efficient GANs, rather than the specific predicted augmentations. Therefore, we believe that our method is generalizable and can be extended to other advanced data augmentations.

**Architectures** We investigate the impact of different network architectures (2-layer multi-layer perceptron (MLP), linear, and bilinear) and input approaches (concatenation  $[\phi(\mathbf{x}); \phi(\hat{\mathbf{x}})]$ , subtraction  $\phi(\hat{\mathbf{x}}) - \phi(\mathbf{x})$ , and augmented samples only  $\phi(\hat{\mathbf{x}})$ ) on AugSelf-GAN. As reported in

Table 8: IS and FID of AugSelf-BigGAN with different architectures and fusions of  $\varphi$  on CIFAR-10 and CIFAR-100 with 10% training data. The best result is **bold** and the second best is underlined. Concatenation means  $[\phi(\mathbf{x}); \phi(\hat{\mathbf{x}})]$ , subtraction means  $\phi(\hat{\mathbf{x}}) - \phi(\mathbf{x})$ , and augmentation means  $\phi(\hat{\mathbf{x}})$ .

Architecture	Input	CIFAR-10 10% data		CIFAR-100 10% data	
		IS ( $\uparrow$ )	FID ( $\downarrow$ )	IS ( $\uparrow$ )	FID ( $\downarrow$ )
2-layer MLP	concatenation	8.54 $\pm$ 0.07	18.47 $\pm$ 0.37	8.65 $\pm$ 0.11	30.15 $\pm$ 0.47
2-layer MLP	subtraction	8.62 $\pm$ 0.07	<u>16.94</u> $\pm$ 0.49	8.88 $\pm$ 0.06	28.63 $\pm$ 0.36
2-layer MLP	augmentation	<u>8.78</u> $\pm$ 0.05	19.06 $\pm$ 0.81	8.73 $\pm$ 0.10	29.40 $\pm$ 0.91
linear	concatenation	<b>8.85</b> $\pm$ 0.11	17.52 $\pm$ 0.20	9.37 $\pm$ 0.09	25.22 $\pm$ 0.25
linear	subtraction	8.76 $\pm$ 0.05	<b>15.68</b> $\pm$ 0.26	<u>9.78</u> $\pm$ 0.08	<b>21.30</b> $\pm$ 0.15
linear	augmentation	8.66 $\pm$ 0.09	20.29 $\pm$ 0.36	<b>9.92</b> $\pm$ 0.10	24.47 $\pm$ 0.58
bilinear	-	8.57 $\pm$ 0.04	25.27 $\pm$ 0.16	9.03 $\pm$ 0.03	26.72 $\pm$ 0.17

Table 9: IS and FID of AugSelf-BigGAN with different loss functions on CIFAR-10 and CIFAR-100 with full and limited training data. The best result is **bold** and the second best is underlined.

Method		100% training data		20% training data		10% training data	
		IS ( $\uparrow$ )	FID ( $\downarrow$ )	IS ( $\uparrow$ )	FID ( $\downarrow$ )	IS ( $\uparrow$ )	FID ( $\downarrow$ )
CIFAR-10	$\lambda_d = 0, \lambda_g = 0$	9.29 $\pm$ .02	8.48 $\pm$ .13	8.84 $\pm$ .12	15.14 $\pm$ .47	8.80 $\pm$ .01	20.60 $\pm$ .13
	$\lambda_d = 1, \lambda_g = 0$	9.12 $\pm$ .05	8.90 $\pm$ .07	8.82 $\pm$ .03	13.65 $\pm$ .70	8.52 $\pm$ .04	18.14 $\pm$ .33
	saturating	9.27 $\pm$ .06	8.13 $\pm$ .14	8.83 $\pm$ .04	12.76 $\pm$ .29	8.42 $\pm$ .05	18.43 $\pm$ .21
	non-saturating	<u>9.37</u> $\pm$ .07	<b>7.60</b> $\pm$ .08	8.91 $\pm$ .09	<u>11.44</u> $\pm$ .16	8.63 $\pm$ .10	<u>15.86</u> $\pm$ .26
	combination	<b>9.43</b> $\pm$ .14	<u>7.68</u> $\pm$ .06	<b>8.98</b> $\pm$ .09	<b>10.97</b> $\pm$ .09	<b>8.76</b> $\pm$ .05	<b>15.68</b> $\pm$ .26
CIFAR-100	$\lambda_d = 0, \lambda_g = 0$	11.02 $\pm$ .07	11.49 $\pm$ .21	9.45 $\pm$ .05	24.98 $\pm$ .48	8.50 $\pm$ .09	34.92 $\pm$ .63
	$\lambda_d = 1, \lambda_g = 0$	10.82 $\pm$ .10	11.29 $\pm$ .12	9.96 $\pm$ .11	18.90 $\pm$ .41	9.45 $\pm$ .05	25.77 $\pm$ .95
	saturating	10.90 $\pm$ .07	10.53 $\pm$ .21	9.71 $\pm$ .08	18.78 $\pm$ .43	9.30 $\pm$ .09	25.92 $\pm$ .12
	non-saturating	<b>11.22</b> $\pm$ .14	<u>9.90</u> $\pm$ .09	<u>10.07</u> $\pm$ .02	<u>16.12</u> $\pm$ .26	<b>9.81</b> $\pm$ .10	<u>21.99</u> $\pm$ .87
	combination	<u>11.19</u> $\pm$ .09	<b>9.88</b> $\pm$ .07	<b>10.25</b> $\pm$ .06	<b>16.11</b> $\pm$ .25	<u>9.78</u> $\pm$ .08	<b>21.30</b> $\pm$ .15

Table 8, we found that more complicated architectures of the backbone  $\varphi$  such as 2-layer MLP with input concatenation ( $\hat{D}(T(\mathbf{x}; \omega), \mathbf{x}) = \text{MLP}([\phi(T(\mathbf{x}; \omega)); \phi(\mathbf{x})])$ ) or bilinear layer ( $\hat{D}(T(\mathbf{x}; \omega), \mathbf{x}) = \phi(T(\mathbf{x}; \omega))^\top W \phi(\mathbf{x})$ ) works worse than the simple linear layer with input subtraction ( $\hat{D}(T(\mathbf{x}; \omega), \mathbf{x}) = W(\phi(T(\mathbf{x}; \omega)) - \phi(\mathbf{x}))$ ), which is the design of AugSelf-GAN. The reason might be that complicated architectures of the head  $\varphi$  actually discourage the backbone  $\phi$  from capturing rich and disentangled representations.

**Generator Loss Functions** We study the effects of AugSelf-GANs with different generator loss functions. As shown in Table 9, The hyper-parameters  $\lambda_d = 0, \lambda_g = 0$  represent the baseline BigGAN + DiffAugment. The generation performance is improved with only augmentation-aware self-supervision for the discriminator ( $\lambda_d = 1, \lambda_g = 0$ ). The saturating version of self-supervised generator loss shows no significant further improvements. The non-saturating version yields comparable performance with the combination one (AugSelf-GAN), and they both substantially surpass the others. The reason is that the non-saturating loss directly encourages the generator to generate augmentation-predictable real data, providing more informative guidance than the saturating one.

## C Computing Resources

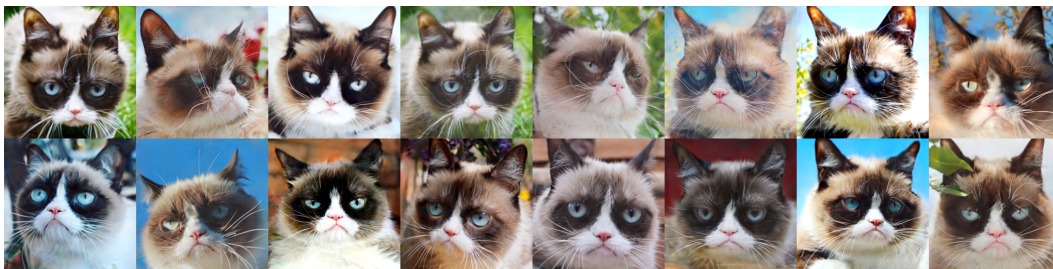
Each of our experiments was conducted using a NVIDIA V100 GPU with memory of 32GB.

## D Generated Images

The following pages show randomly generated images of AugSelf-GAN (and AugSelf-GAN+) trained on the low-shot datasets (Figure 6), FFHQ (Figures 7 and 8), and LSUN-Cat (Figures 9 and 10).



(a) Obama



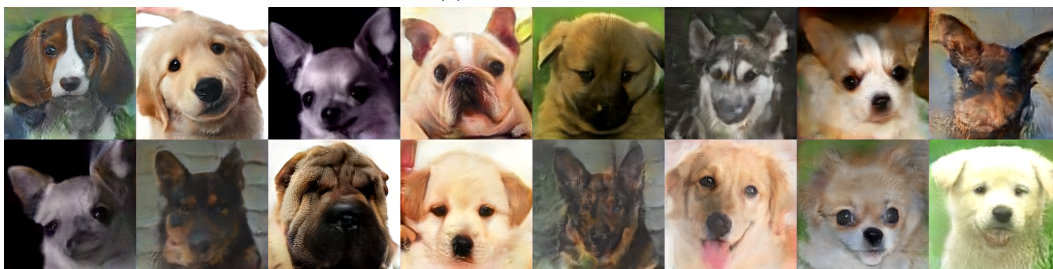
(b) Grumpy cat



(c) Panda



(d) AnimalFace cat



(e) AnimalFace dog

Figure 6: Randomly generated images of AugSelf-StyleGAN2 on five low-shot datasets.





(a) 1k training samples



(b) 5k training samples



(c) 10k training samples



(d) 30k training samples

Figure 7: Randomly generated images of AugSelf-StyleGAN2 on FFHQ.





(a) 1k training samples



(b) 5k training samples



(c) 10k training samples



(d) 30k training samples

Figure 8: Randomly generated images of AugSelf-StyleGAN2+ on FFHQ.





(a) 1k training samples



(b) 5k training samples



(c) 10k training samples



(d) 30k training samples

Figure 9: Randomly generated images of AugSelf-StyleGAN2 on LSUN-Cat.





(a) 1k training samples



(b) 5k training samples



(c) 10k training samples



(d) 30k training samples

Figure 10: Randomly generated images of AugSelf-StyleGAN2+ on LSUN-Cat.